NANOTOPOGRAPHIC CONTROL OF HUMAN EMBRYONIC STEM CELL FUNCTION

W. Chen[1], Y. Sun[1] and J. Fu[1, 2] *

[1]Department of Mechanical Engineering and [2]Department of Biomedical Engineering, University of Michigan, Ann Arbor, MI USA

ABSTRACT

Human embryonic stem cells (hESCs) exhibit diverse behaviors responding to their microenvironment. Here we developed an effective method for precise control of local nanoroughness on glass substrates using the reactive ion etching (RIE) and photolithography techniques. We for the first time demonstrated that the local nanoroughness could mediate hESC functions, including morphology, attachment, proliferation and differentiation.

KEYWORDS: Human Embryonic Stem Cell, Nanotopography, Nanoroughness, Extracellular Matrix.

INTRODUCTION

Human embryonic stem cells (hESCs) have attracted much attention given their pluripotency and potential therapeutic applications [1-2]. It is well-known that soluble factors are critical in regulating their function, yet how the physical cues in cell microenvironment, such as surface nanoroughness, regulate functions of hESCs remain elusive and largely uncharacterized [3-6]. In this work, we proposed a microfabrication method to achieve a precise control of local nanoroughness on glass substrates. We successfully demonstrated that hESCs and NIH/3T3 fibroblasts had high sensitivity and exhibited diverse and cell-type specific responses to nanotopography.

RESULTS

Local nanoroughness was defined on glass substrates via photolithography and RIE (Fig. 1A). By precisely controlling photolithography and RIE etching, we could specify location, shape, area and roughness level (characterized using root mean square roughness or R_{RMS}) of different nanorough islands on glass substrates (Fig. 1B-E). Using nanorough glass surfaces, we studied responses of hESCs to different levels of nanoroughness R_{RMS}. First, on patterned nanorough surfaces, hESCs appeared to selectively adhere to and aggregated on the smooth area (R_{RMS} = 1 nm) as compared to the nanorough surface (R_{RMS} = 70 nm) after plating for 24 hrs (Fig. 2A). Adhesion rates of hESCs on the smooth (R_{RMS} = 1 nm) and nanorough (R_{RMS} = 70, 150 nm) substrates after plating for 24 hrs were quantified and compared in Fig. 2B. Our results suggested that regardless of treatment with Y27632 (a contractility inhibitor commonly used to enhance survival of hESCs), hESCs had a greater adhesion rate on the smooth surface. Further, Fig. 2C&E showed the smooth glass surface was supportive for long-term culture of undifferentiated, pluripotent hESCs, as indicated by a higher percentage of hESCs positively expressing OCT 3/4 after 7 days of culture on the smooth glass surface as compared to the nanorough ones. Next, the cell population doubling time of hESC colonies on smooth and nanorough glass surfaces were examined (Fig. 2D&F). hESCs proliferated faster with a shortened doubling time on the smooth surface as compared to the nanorough ones. Morphological analysis using scanning elec-

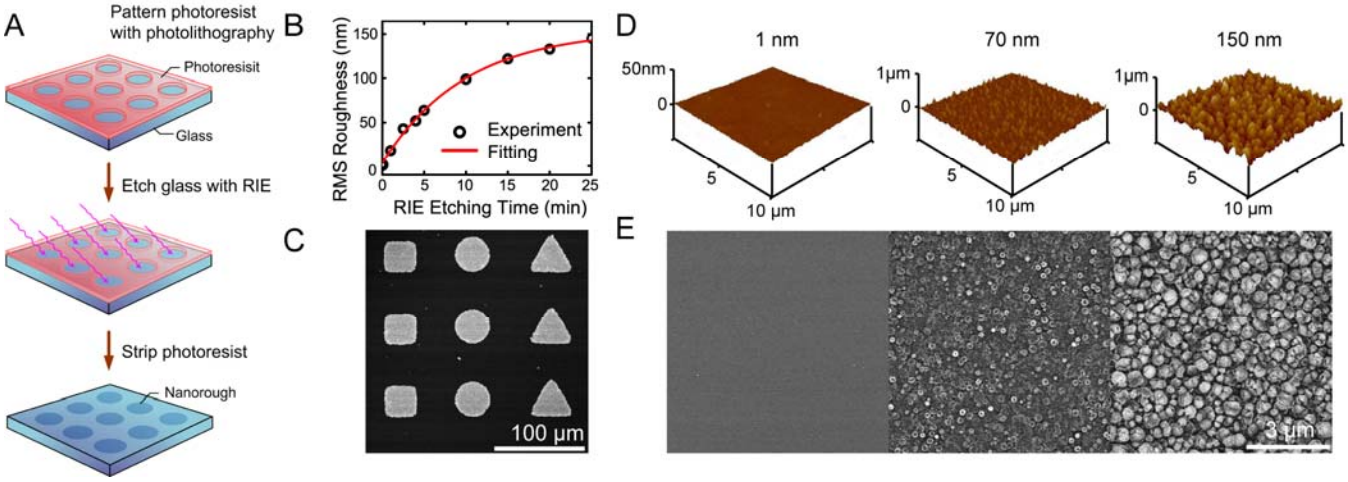

Figure 1: Substrates fabrication and characterization. (A) Schematic of fabrication process for the nanorough substrate. (B) Substrate roughness plotted against RIE etching time. (C) SEM image of a glass substrate micropatterned with nanorough (70 nm) islands. (D) AFM and (E) SEM topographs of glass substrates with nanoroughness of 1 nm, 70 nm and 150 nm.

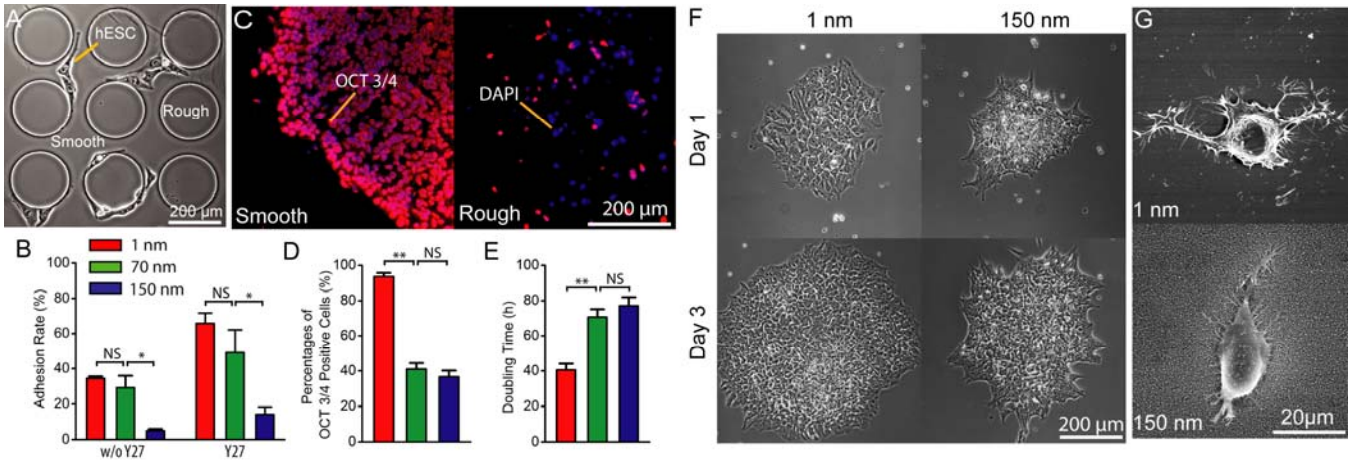

Figure 2: hESC behaviors on smooth and nanorough glass substrates. (A) Phase image of hESCs selectively attach to the smooth (R_{RMS} =1 nm) surface of the micropatterned substrate rather than the nanorough (R_{RMS} =70 nm) islands after plating for 24 hrs. (B) Adhesion rates of hESCs on the smooth and nanorough glass substrates after plating for 24 hrs, with treatment with Y27632. (C) Percentages of OCT 3/4 positive hESCs and on the smooth and nanorough glass substrates after plating for 7 days. (D) Cell population doubling time of hES colonies on smooth and nanorough glass substrates. (E) Immunofluorescence images of hESCs cultured 7 days on smooth (R_{RMS} =1nm) and nanorough (R_{RMS} =150nm) substrates showing expression of hES cell markers (OCT3/4, pink color) and stained Nuclei (DAPI, blue color). hESCs have a higher tendency to differentiate on rough surface. (F) Representative phase images of hESC colonies on smooth (R_{RMS} =1 nm) and nanorough (R_{RMS} =70 and 150 nm) substrates after plating for 1 day and 3 days. (G) SEM images of hESCs on smooth and nanorough substrates after plating for 24 hrs.

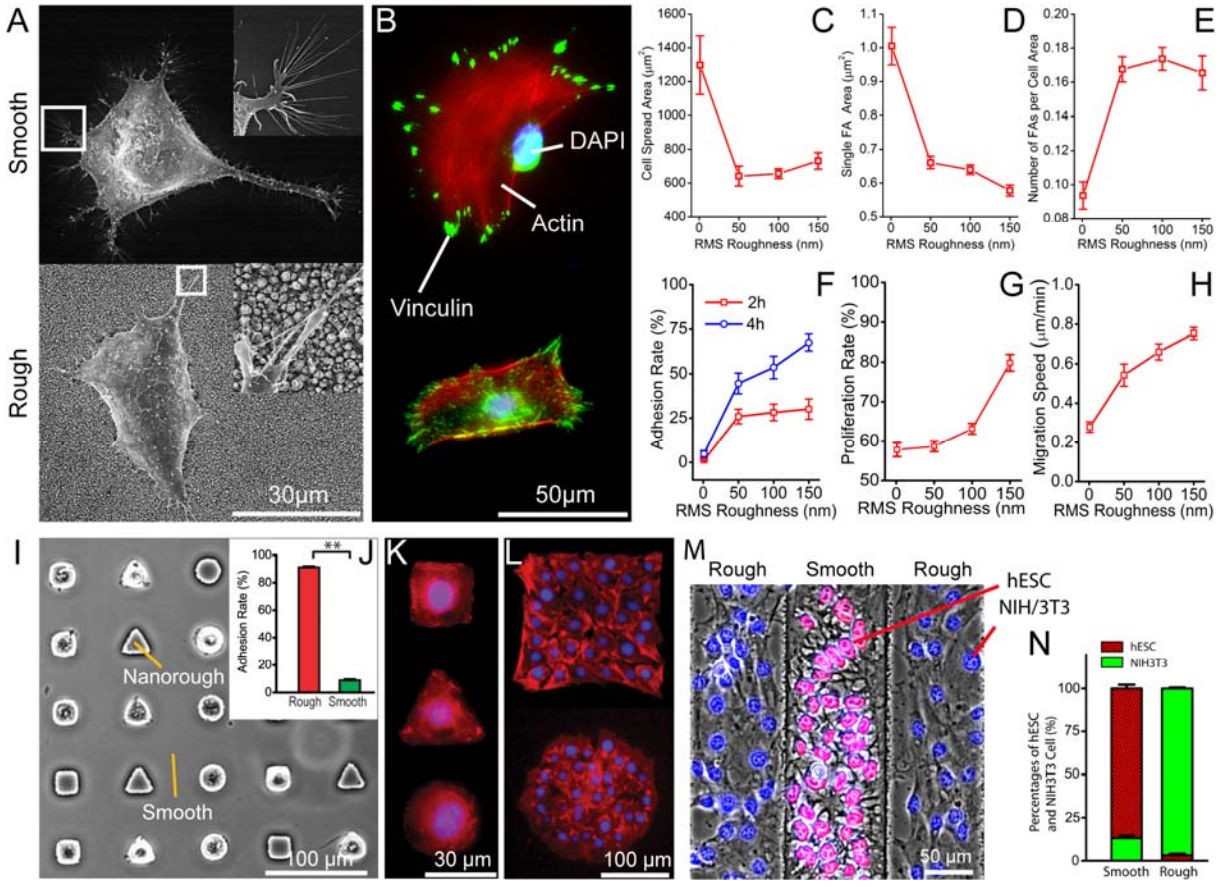

Figure 3: NIH/3T3 cell behaviors on smooth and nanorough glass substrates. (A) SEM and (B) immunofluorescence images of stained NIH/3T3 fibroblasts on smooth (R_{RMS} =1 nm) and nanorough (R_{RMS} =150 nm) substrates. (C) Cell spreading area,

(D) single FA area, (E) number of FAs per cell area, (F) cell adhesion rate, (G) proliferation rate and (H) migration speed as functions of nanoroughness for NIH/3T3 fibroblasts. (I) Phase image, (J) cell adhesion rate and (K) immunofluorescence images of NIH/3T3 fibroblasts on micropatterned nanorough (R_{RMS} =70 nm) islands, 4 hrs after initial cell seeding. (L) Immunofluorescence images of fibroblasts colonies on patterned nanorough islands, 48 hrs after initial cell seeding. Cells are stained with the nuclear maker DAPI (blue) and phalloidin to visualize F-actin filaments. (M) Merged phase and immunofluorescence image and (N) quantified results of hESCs and NIH3T3 cells selectively attach to and aggregated on the smooth (1nm) and nanorough (70 nm) surfaces of the micropatterned nanorough substrate after plating for 48 hrs in StemPro medium with Y27632, showing expression of hES cell markers (OCT3/4, pink color) and stained Nuclei (DAPI, blue color).

-tron microscopy (SEM) showed that hESCs demonstrated more filopodia structures on the smooth surface as compared to the nanorough ones. Taken together, we proved for the first time that nanoroughness could be a potent physical signal in cell microenvironment to regulate hESC stemness maintenance and proliferation.

Cellular responses to nanoroughness could be cell-type specific [7-8]. Fig. 3A-H showed that NIH/3T3 demonstrated smaller spread area and more filopodia structures, greater attachment and proliferation rates, and faster migration on the nanorough surfaces as compared to smooth controls. Prominent focal adhesions (FAs; visualized by staining for FA protein vinculin in Fig. 3B) were distributed primarily on the periphery of the cells plated on the smooth surfaces, while for cells on the nanorough substrates, punctuate adhesion structures of smaller sizes and a greater density were randomly distributed over the entire cell. These punctuate adhesions suggested fast FA turnover and weak actomyosin contraction, which could lead to disorganized actin filaments and rapid cell migration as we had observed. We further used micropatterned nanorough surfaces to modulate spatial locations of cell attachment, single cell and cell colony shape for NIH/3T3. The nanorough islands showed an extremely high selectivity for attachment of NIH/3T3 (Fig 3I-L). About 91% of NIH/3T3 were preferentially attached to the nanorough islands and the cell and colony spreading were also confined by the shapes of nanorough islands. Lastly, we demonstrated in Fig. 3M-N that on smooth glass surfaces with nanorough petterns, after plating for 48 hrs, co-cultured hESCs and NIH/3T3 could selectively attach to different areas of the patterned surfaces, and the two cell types were spatially segregated based on their cell-type specific preference for nanoroughness.

CONCLUSION

Our study here provided a simple strategy to generate local nanotopography and demonstrated controls of cell morphology, attachment, growth, differentiation, cell and colony spreading of hESCs and NIH/3T3 on glass substrates patterned with surface nanoroughness. Our work could be useful for understanding the physical regulation of hESC functions, which has so far remained largely uncharacterized. Our micropatterned nanorough surfaces might find additional uses in applications such as cell separation and cell coculture.

ACKNOWLEDGEMENTS

We acknowledge financial support from the department of mechanical engineering at University of Michigan. This work used the Lurie Nanofabrication Facility at the University of Michigan, a member of the National Nanotechnology Infrastructure Network (NNIN) funded by the NSF.

REFERENCES

[1] G. Q. Daley and D. T. Scadden, *Prospects for stem cell-based therapy*, Cell **132**, 544-548 (2008).
[2] G. Keller, *Embryonic stem cell differentiation: emergence of a new era in biology and medicine*, Genes & Development **19**, 1129-1155 (2005).
[3] L. A. Johnston, *Competitive interactions between cells: death, growth, and geography*, Science **324**, 1679-1682 (2009).
[4] S. J. Morrison and A. C. Spradling, *Stem cells and niches: mechanisms that promote stem cell maintenance throughout life*, Cell **132**, 598-611 (2008).
[5] D. L. Jones and A. J. Wagers, *No place like home: anatomy and function of the stem cell niche*, Nature Reviews Molecular Cell Biology **9**, 11-21 (2008).
[6] D. T. Scadden, *The stem-cell niche as an entity of action*, Nature **441**, 1075-1079 (2006).
[7] M. M. Stevens and J. H. George, *Exploring and engineering the cell surface interface*, Science **310**, 1135-1138 (2005).
[8] A. Curtis and C. Wilkinson, *Topographical control of cells*, Biomaterials **18**, 1573-1583 (1997).

CONTACT

*J. Fu, jpfu@umich.edu